IJCRT.ORG ISSN : 2320-2882

INTERNATIONAL JOURNAL OF CREATIVE RESEARCH THOUGHTS (IJCRT)

An International Open Access, Peer-reviewed, Refereed Journal

Influence Of Heat Input On Weld Microstructure And Mechanical Properties Of TIG Welded Al-4043 WAAM Alloy

M Akash, S Shashi Kumar*, Hemanth Kumar M S, Sujith B, Subhash M, Muralidhar M,

Department of Metallurgical and Materials Engineering, Jain University, Bengaluru 562112.

Abstract:

WAAM is a form of Direct Energy Deposition that 3D prints metal parts using an arc welding process. Unlike other conventional AM methods, WAAM uses an electric arc to melt metal wire. The procedure is guided by a robotic arm, where the shape of the product is created on a substrate material. When the wire is melted, it is extruded into beads on the substrate. The beads bind together, forming a coating of metal. The process is repeated in a layer-by-layer fashion until the required metal part is finished.

In the present study, a rectangular slab of dimensions 300 x 200 x 20 mm^3 was fabricated using 4043 MIG filler wire via wire arc additive manufacturing (WAAM). The effect of welding current (heat input) on the weld microstructure and mechanical properties of 4043 WAAM alloy was investigated. Three weld joints were produced by varying the welding current from 140 to 160 A for the other welding parameters kept at constant value. The experimental findings reveal that all the weld joints were defect free and the strength of the weld decreased for the increase in the welding current. A highest joint strength of 120 MPa (119% of the base WAAM strength) was achieved in case of lower heat input(140A) weld joint. The significant strength is due to presence of more refined equiaxed dendritic microstructure and smaller size of fusion boundary. The toughness of the weld joints were 10, 11 and 12 Joules for low, medium and high heat input respectively. The toughness of the weld joints shows an increasing trend for the increase in the welding current. More softening of the weld joint has resulted in higher ductility and toughness. The results of pitting corrosion studies reveal that overall, a better and similar corrosion behaviour was achieved in all the weld joints, owing to presence of more Si in the Al matrix. The difference in the heat input and grain coarsening in the weld microstructure has attributed to variation in the corrosion resistance of the weld joints. However, the corrosion resistance of the weld joints are within the acceptable limit of the industry standards.

Keywords: CMT- WAAM, Aluminium alloys, Pore, Microstructure, Tensile properties.

1. Introduction

Al 4043 Aluminium alloy is Al-Si alloy with good corrosion resistance typically used as a filler wire material with good fluidity and produce less defects [1]. Al 4043 is less sensitive to weld cracking and is recommended for welding of both heat treatable and non-heat treatable aluminium alloys. 4043 alloy possesses good toughness and higher ductility. The presence of silicon in 4043 alloy offers good strength to weight ratio and improves fluidity during welding [2]. Aluminium alloys are used in electronic technology, automobile body structure, wind and solar applications, marine and aerospace industries. Al 4043 is mainly used as a filler wire to weld aluminium alloy parts [3].

Additive manufacturing (AM), is a direct energy deposition method, which uses data from computer-aided-design (CAD) software to fabricate parts in a layer by layer and opens up new possibilities for advanced manufacturing. The AM technique has been used to effectively create a variety of aluminium parts and structures including ally combination of Al-Si, Al-Si-Mg, Al-Zn-Mg-CU, and Al-Cu alloys. Powder bed fusion, Electron beam melting, selective laser sintering etc., are the some of well-known powder-based methods in additive manufacturing [4-5]. These methods often experience problems related to high porosity low surface quality, uncontrolled grain growth material loss through evaporation, high operating cost and anisotropic microstructure during material deposition [6]. AM using wire arc can be a promising method for fabrication of 3D metal parts. Direct energy deposition assists in melting of the wire and depositing on the substrate material. The process offers high rate of deposition and cheap operating cost when compared to powder based metals. Fabrication of 3D metal parts using GMAW- WAAM and GTAW-WAAM are available in the literatures[7].

Due to the continuous arc maintained by the tungsten electrode and the filler wire in GMAW requires more heat input and causes grain coarsening due continuous heat transfer. The metal deposition rate of GMAW-WAAM and GTAW-WAAM are 3-4kg/hr and 1-2kg/hr respectively. Where CMT-WAAM has a deposition rate of 3.6kg/hr with low heat input. CMT based WAAM process have better mechanical and metallurgical properties than GTAW-WAAM and GMAW-WAAM [14].

WAAM using GMAW and GTAW are most widely used in many applications. The problems with respect WAAM based on Cold metal transfer (CMT) is an economical and rapid prototyping method for high quality metal parts digitally through continuous surfacing, which uses arc as the heat source to fuse the work [7]. The major problems associated in WAAM are residual stresses and heat input distortion – deformation caused by residual are a major cause of tolerance loss in WAAM and therefore difficulties in controlling dimensional accuracy specially in large parts The WAAM involves a high periodic heat input due to the process of arc welding. In WAAM, solidification poses significant challenges in processing materials due to the promotion of a large-grain microstructure. The effect of long periods of high temperatures in WAAM have specific constraints to the degree of precision that can be achieved in the deposition process. However, the problems can be overcome through CMT-WAAM where heat accumulation can be controlled. CMT-WAAM process not only include lower thermal input with alternation in electrode burn-off rate but also great control over the penetration with high wire melting sufficiency and high deposition rate comparable to WAAM [8-13].

Miao et al.(2020) reported on comparative study of microstructure evaluation and mechanical properties of 4043 aluminium alloy fabricated by wire-based additive manufacturing After adding laser energy, the tensile strength, yield strength, and elongation after the input of laser energy are 163.39 MPa, 75.60 MPa, and 17.38 percent, respectively, which are 7.56 percent, 8.45 percent, and 3.45 percent greater than before. The finer gains, reduced Si segregation, and crack deflection are responsible for the improved mechanical characteristics.

Gu et al.(2015) studied on wire arc additive manufacturing of aluminium investigated that Standard and new feedstock compositions are being evaluated and developed with ultimate tensile strengths of up to 260 MPa with 17% elongation being obtained in the as-deposited condition resulting in refined equiaxed microstructure and elimination of porosity.

Ortega et al.(2019) investigated on Characterisation of 4043 aluminium alloy deposits obtained by wire and arc additive manufacturing using a Cold Metal Transfer process, formed microstructures were analysed and the porosity defects were quantified and discussed with regard to the heat input characteristics and the solidification conditions.

Vishnukumar et al.(2021) reported on Wire arc additive manufacturing for repairing aluminium structures in marine applications in which aluminium filler material ER4043 was deposited on AA5052 using Cold metal transfer (CMT) process-based Wire arc additive manufacturing (WAAM) technology. The microstructural evolution of WAAM processed plates via CMT, and CMT + Pulse (CMT + P) modes were investigated. The microstructure of CMT + P mode revealed fine equiaxed dendrites in comparison to CMT mode. Energy Dispersive X-Ray Spectroscopy (EDS) elemental maps and line scan revealed the presence of Al-Si eutectic phase. The corrosion rate of WAAM processed samples (0.18–0.20 mm/year) was comparable with the wrought counterparts (0. 19–0.21 mm/year).

Xuewei Fang et. al., worked on Microstructure evolution of wire arc additively manufactured 2319 aluminium alloy with interlayer hammering. Fabrication of 2319 Al alloy by CMT-WAAM was performed. Samples were investigated to evaluate the effects of inter layer deformation. Grain size distribution and internal sub-microstructure were examined by TEM. Results of higher yield strength, ultimate tensile strength and fine grain size have been obtained.

Yueling Guo et.al., studied on Comparative Study on Wire-Arc Additive Manufacturing and Conventional Casting of Al–Si Alloys: Porosity, Microstructure and Mechanical Property. Fabrication of 4047 Al-Si alloy by WAAM was carried out. X-ray microscopy reveals that WAAM causes a higher volume fraction of gas pores in comparison with conventional casting. Effective refinements of α-Al dendrites, eutectic Si particles and Fe-rich intermetallic compounds are achieved by WAAM, resulting from its rapid solidification process.

Xuewei Fang et. al., performed on Microstructure evolution and mechanical behavior of 2219 aluminum alloys additively fabricated by the cold metal transfer process. Four different welding arc modes including conventional cold metal transfer (CMT), CMT-Pulse (CMT-P), CMT-Advanced (CMT-ADV), and CMT pulse advanced (CMT-PADV) were used to deposit 2219-Al wire. The effects of different arc modes on porosity, pore size distribution, microstructure evolution, and mechanical properties were thoroughly investigated. CMT-PADV process gave the smallest pore area percentage and pore aspect ratio, and had almost no larger pores. Mechanical properties of 2219 aluminum alloy was improved using the CMT-PADV arc mode.

Zewa Qi et. al., worked on Microstructure and mechanical properties of wire arc additively manufactured Al-Mg-Si aluminium alloy. Fabrication of Al-Mg-Si aluminium alloy by WAAM was carried out. Filler materials used was ER5087(Al-5Mg) and ER4043(Al-5Si) wires. The result had the phase of α-Al, Mg-Si and Al-Si was distributed along the grain boundary. The properties in vertical direction were lower than horizontal direction.

2. Experimental Details

2.1 Experimental setup and materials

To manufacture the Al–Si plate component, Al-4043 filler wire with a 1.2 mm diameter was used. The chemical composition of the filler wire used in this study is presented in Table 2.2, and the mechanical properties of the filler wire is given in table 2.1. A welding power source (The Kuka KR15 TPS4000) was used which was a 6-axis automated system and work table was made stationary using the WAAM technique (shown in fig 2.1). The Al-4043 filler wire was deposited on the aluminium alloy plate substrate, the component is shown in fig 2.2

Table 2.1 Mechanical properties of 4043 aluminium wire.

PROPERTIES	ULTIMATE TENSILE STRENGTH (MPA)	YIELD STRENGTH(MPa)	% OF ELONGATION	DENSITY (g/cc)	HARDNESS (VHN)
4043 aluminium	120	40	7	2.7	87

Table 2.2 Chemical composition of 4043 Al alloy in (Wt%) :

Al	**Si**	**Fe**	**Cu**	**Mn**	**Zn**	**Mg**	**Ti**	**Be**	**Others**
Balance	4.5-6	0.8	0.3	0.05	0.10	0.05	0.20	0.0008	0.15 max

The CMT-WAAM fabrication system, which is depicted in Fig.2.1, was used in the current work to fabricate aluminium walls from wire produced of the 4043aluminium alloy. The KUKA KR15 (TPS4000 MIG MAG Welding) Robotic machine used the CMT Advanced technology to fabricate 4043 aluminium plate. This device was a 6-axis robot. When one parameter is changed, the others follow suit. The shielding gas was 15 L/min of pure argon (99.99%) at a steady flow rate. The contact tip to work distance (CTWD) was maintained at 15 mm. Walls were constructed utilising all four CMT process variations at wire feed speeds (WFS) of 5.3 m/min, 12 volts, and currents of 76 amps, with dimensions of 300 mm in length and 200 mm in height. By moving from right to left and left to right, it creates a layer with a height of 2.3mm in one pass. 16kg was the sustained pay load. The CMT-WAAM process parameters are given in table 2.3.

Table 2.3 CMT WAAM Parameters

Wire Dia	Wire Feed Rate	Voltage	Current	Inert gas flow rate	Height of one layer	Pay load
1.2mm	5.3m/min	12V	76amps	15ltr/Min	2.3mm	16Kg

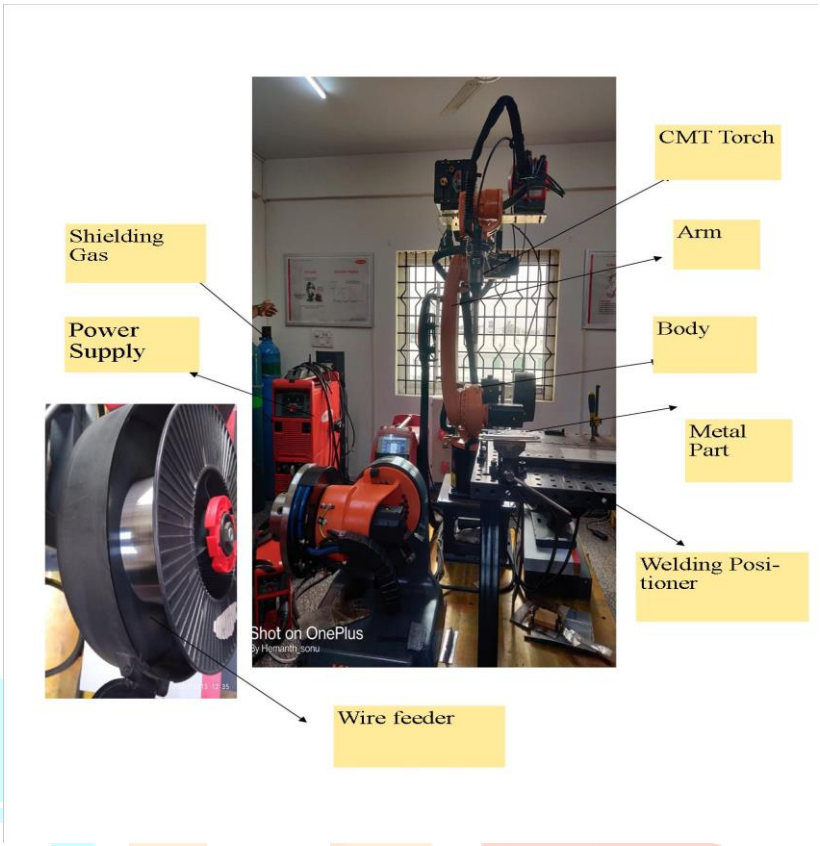

Fig.2.1: KUKA KR15 ROBOT

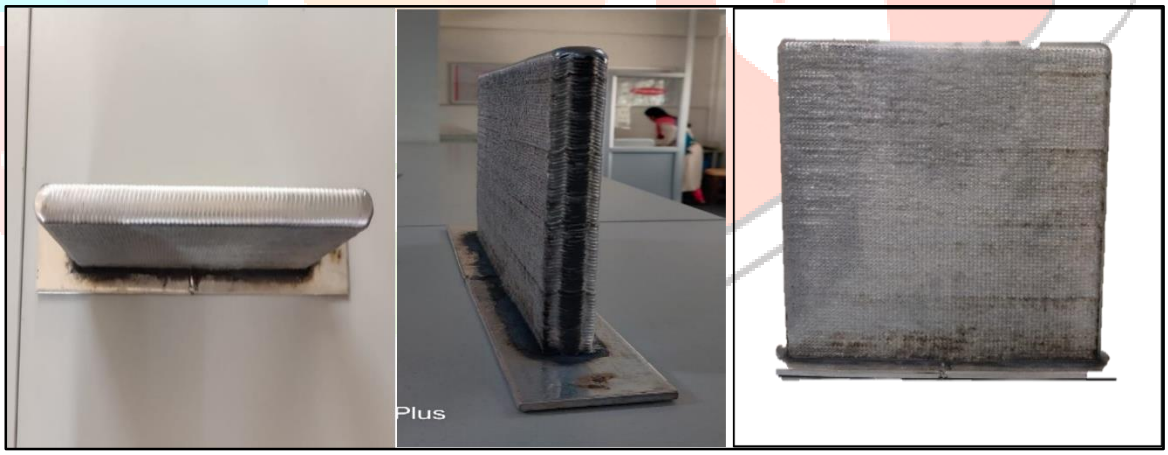

Fig 2.2 Photograph of the fabricated component (300mm*200mm*15mm)

2.2 Plates Extraction for TIG welding

A total of six samples were extracted from the fabricated part for TIG welding of dimensions 100*50*6 by electrical discharge machine (EDM).

Fig 2.3 Extracted samples for TIG welding

2.3 Plates Preparation

The TIG samples were V-grooved to obtain deeper weld penetration.

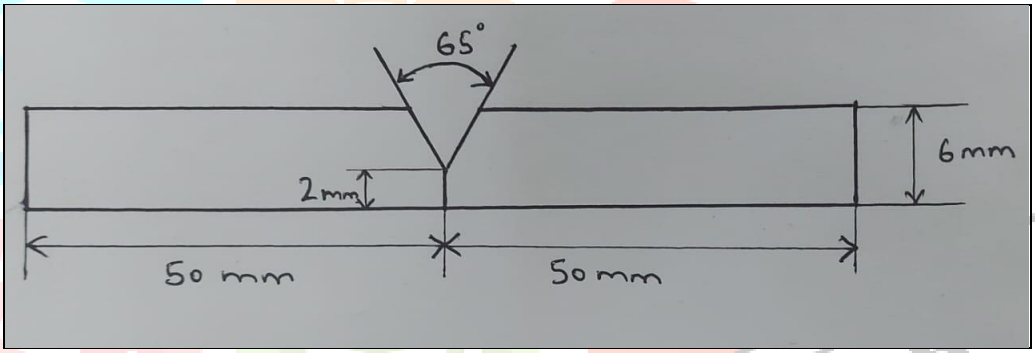

Fig 2.4 Dimensions for V-groove cutting

2.4 TIG Welding parameter

Table 2.4 Tig welding parameter

Parameters	Sample 1	Sample 2	Sample 3
Current (Amps)	150	140	160
Voltage (V)	10.7	10.7	10.7
Travel speed (m/s)	1.09	1.09	1.09
Argon gas flow rate (ltr/mm)	20	20	20
Heat input (KJ/mm)	1.25	0.962	1.5

Fig 2.5 TIG welded samples

3. Results and Discussion

3.1 Evaluation of tensile Properties of TIG welded joints

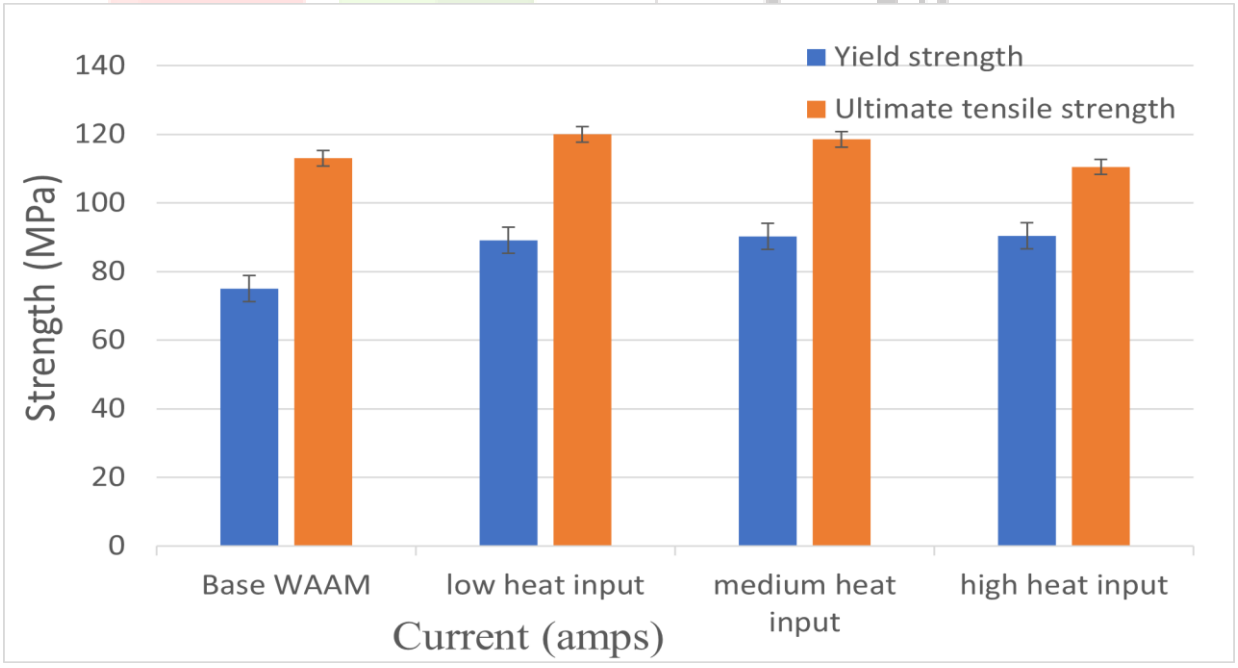

Fig 3.1 Tensile properties comparison graph of TIG weld zone and WAAM alloy

Fig 3.1 shows that the tabulated tensile properties of WAAM and TIG welded joints for varying heat input. The base WAAM has a yield and Ultimate tensile strength of 75 and 113MPa respectively. The yield and Ultimate tensile strength of TIG welded joints at low, medium and high heat input was 89, 80 and 75 and 120, 118 and 110 respectively. It is observed that the yield and ultimate tensile strength of the joints decrease with increase in heat input. A higher strength of 120MPa (greater than the ultimate tensile strength of base WAAM) is achieved at lower heat input. The presence of more equiaxed dendritic grains, smaller fusion boundary and negligent coarse of grain in heat affected zone has attributed towards achieving a relatively higher strength in the weld joint. It is observed that the fracture has been occurred on base metal.

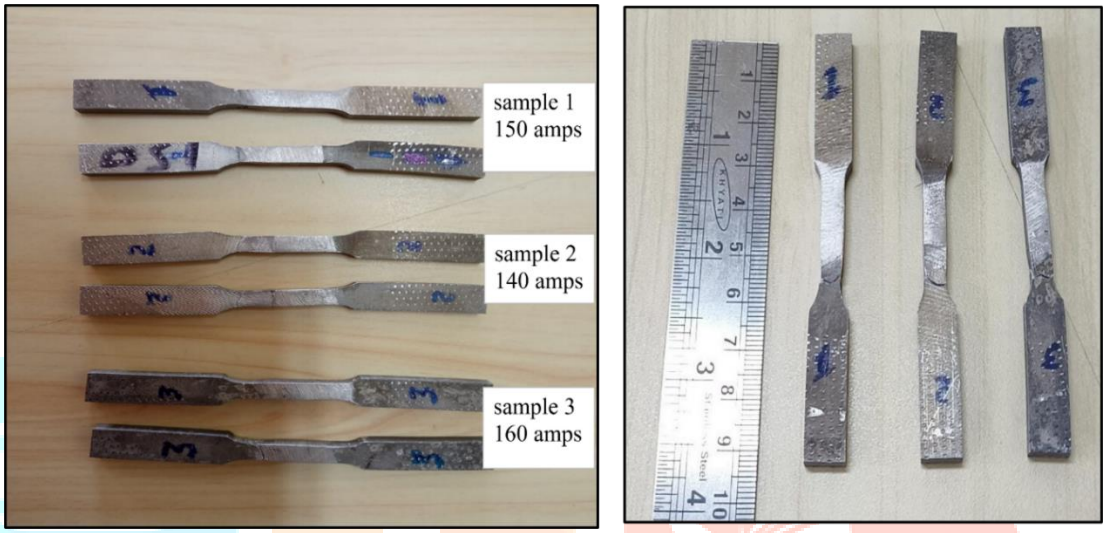

Fig 3.2 Tensile specimen before and after test

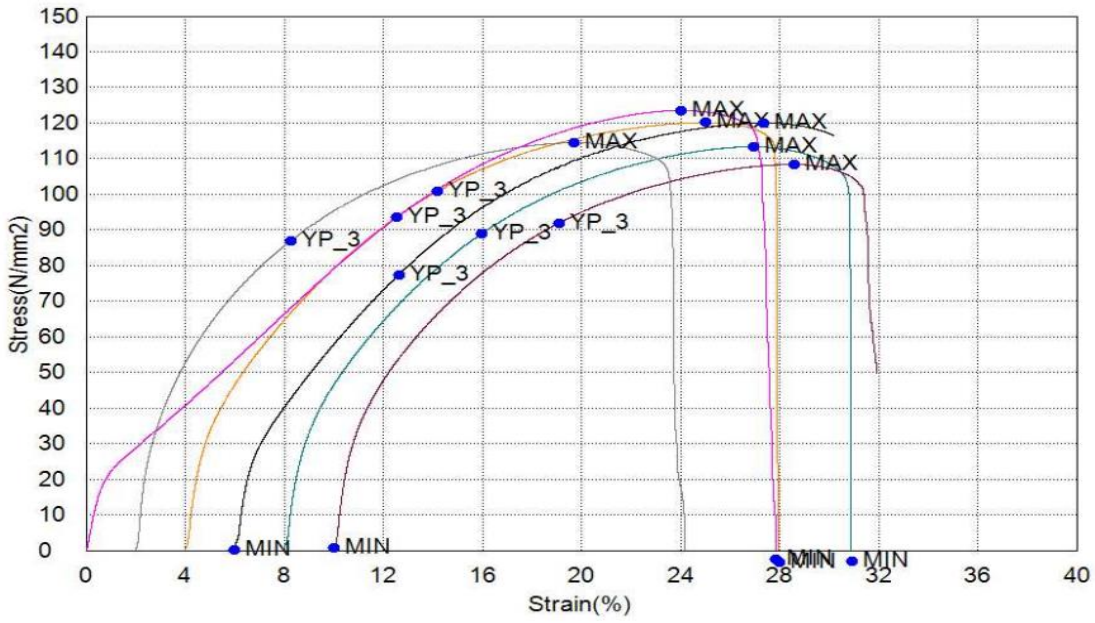

Fig 3.3 Stress v/s strain graph of weld zone

3.2 Evaluation of Toughness (Charpy Test)

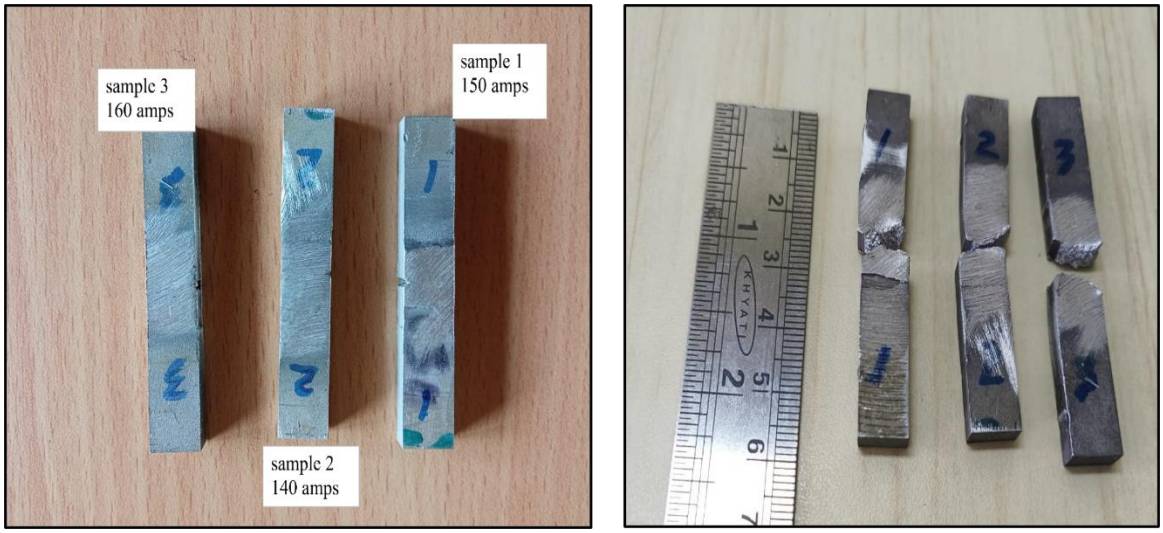

Fig 3.4 Charpy specimen before and after test

The Charpy test of the samples were performed at room temperature condition. It was found that the toughness of TIG weld joints were 10, 11, and 12J for low, medium and high heat input respectively. Whereas, the toughness of the base WAAM alloys was 15Joules. The result indicates that the toughness increases with increase in heat input.

3.3 Microstructure Analysis

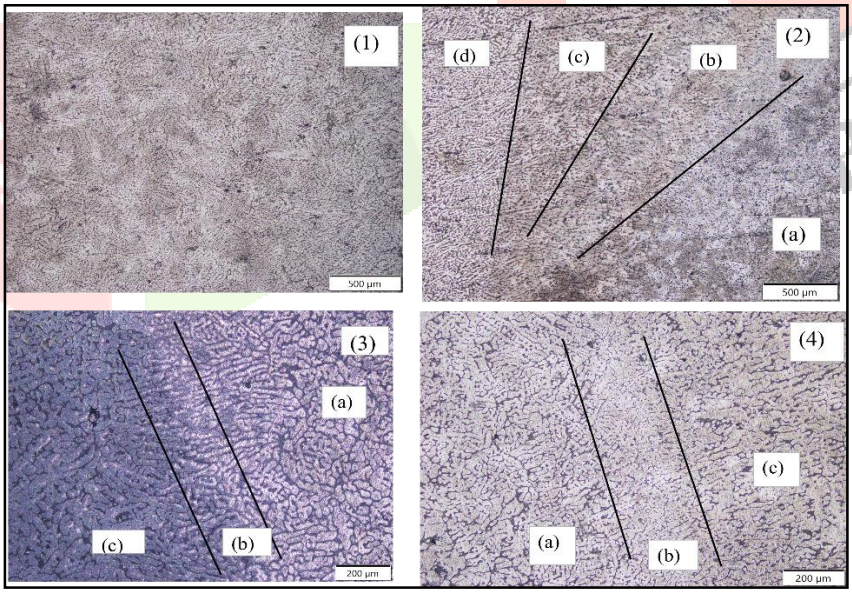

Fig 3.5 Optical images of (1)-WAAM, (2)(3)(4)-weld zones of 140,150 and 160 amps respectively. (a)-weld nugget (b)-fusion zone (c)-heat affected zone (d)-unaffected parent metal.

The fig 3.5 shows the optical microscopic image of the WAAM and TIG welded WAAM joints. The weld zone of TIG welded joint comprises of the heat affected zone and un-affected base metal. The microstructure of base WAAM compress of equiaxed and dendritic grains. At the weld joint interface various grains morphology such as columnar, dendritic and equiaxed grains are observed. The size of the weld B increases

with increase in the heat input as a result at the centre of the weld nugget the size of equiaxed dendritic grain is larger also the size of the fusion boundaries increases with increase in heat input due to significant melting and nucleation of partially melted grains. Because of high exposure of heat and slow cooling rate in the weld nugget at high heat input (160 amp) tig welded joint, the area of recrystallization increased and the grain were coarsened in the heat affected zone(HAZ). Where as in case of low heat input (140 amp) and medium heat input (150 amp) TIG welded joints the lower peak temperature and faster cooling rates in the weld joints, decreased the size of the diffusion boundary and improved grain stability.

It was also interesting to observe that within the weld nugget, different grain morphologies such as cellular, equiaxed, and columnar dendritic grains were observed. The complex microstructure was due to high thermal gradients during welding, which resulted in non-equilibrium conditions during rapid solidification. The grain size of the weld nugget was influenced by the product of the G*R ratio, while the grain morphology in the weld nugget was influenced by the G:R ratio, were G was the thermal gradient and R was the rate of solidification. It is observed that during slow cooling rates, the columnar grains grew and were perpendicular to the direction of the weld boundary from either side of the weld pool, while at higher cooling rates, the columnar grain grew perpendicular the direction of the weld boundary from either side of the weld pool that met the equiaxed grains grown at the weld centre during solidification. Generally, planar growth occurs when G was very high or/and r was very low. As R increased, solidification morphology could shift to the cellular, columnar and then equiaxed dendritic. Cellular and columnar growth modes were produced when the growth of crystal structures occurred without the formation of any secondary dendrite arms. When additional dendritic arms are formed, equiaxed morphology was possible only when G was very low. As the cooling rate of the liquid in front of the solidification boundary (which is the product of G and R) increased, it resulted in a finer dendritic solidification microstructure. Eventually, the finer microstructure leads to the improved mechanical properties of the metals.

3.4 Pitting corrosion test

Table 3.1 corrosion test

Sample no	Current amps	E corr	I corr	Corrosion rate(mm/year)
1	150	-700.06	1.4176	0.0154
2	140	-709.17	1.3668	0.014
3	160	-822.96	1.4552	0.015

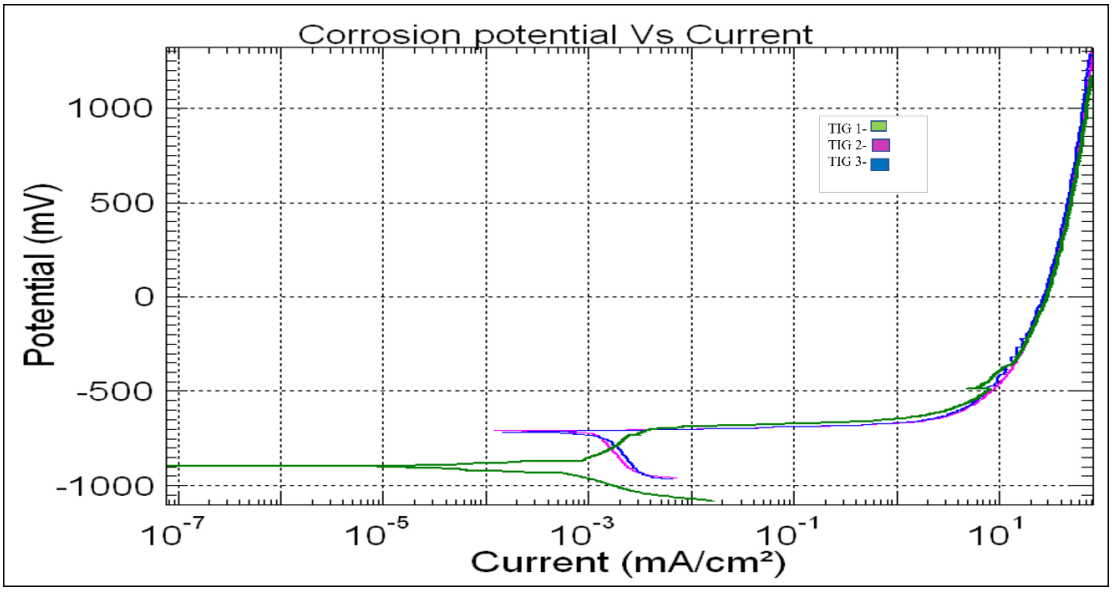

Fig 3.6 Tafel plot exploration of TIG welded joints

Pitting corrosion resistance of TIG welded Al 4043 WAAM alloy was studied using single loop cyclic polarization test. The Tafel plot is generated and the salient features such as corrosion potential, corrosion current density and pitting potential was recorded during the study. Fig. 3.6 illustrates a typical Tafel plot generated between Log I v/s Potential. It is founded that the over all corrosion resistances of TIG welded joints are with in the industrial standards. This is due to the higher concentration of Silicon which is disposed in to α-Al matrix also it is clear from misconstrue studies that low heat input weld joints was composed of equiaxed dendritic structure which improved the strength and corrosion resistance in the weld joint. The less number of Pitts on the corroded surface and the intensity it is also a indication of lower corrosion resistance in the welded samples.

Conclusion:

In the present study, the effect of welding current on weld microstructure and mechanical properties of Al-4043 WAAM alloy was investigated.

The following are the key conclusions.

- Defects free welds were produced during TIG welding of 4043 WAAM alloy.
- The heat input had a significant effect on strength and toughness.
- The strength of the weld joint decreases with increase in welding current and a higher strength of 120MPa was achieved.
- The toughness of the weld increases with increase in the weld current.
- Overall, a better pitting corrosion resistance was achieved and trend was similar for all the weld joints.

References

1. Miao, Qiuyu, et al. "Comparative study of microstructure evaluation and mechanical properties of 4043 aluminium alloy fabricated by wire-based additive manufacturing." *Materials & Design* 186 (2020): 108205.
2. Heidarzadeh, Akbar, et al. "Friction stir welding/processing of metals and alloys: a comprehensive review on microstructural evolution." *Progress in Materials Science* 117 (2021): 100752.
3. Varshney, Deekshant, and Kaushal Kumar. "Application and use of different aluminium alloys with respect to workability, strength and welding parameter optimization." *Ain Shams Engineering Journal* 12.1 (2021): 1143-1152.
4. https://www.ge.com/additive/additive-manufacturing
5. Jiménez, Mariano, et al. "Additive manufacturing technologies: an overview about 3D printing methods and future prospects." *Complexity* 2019 (2019).
6. Singh, Sudhanshu Ranjan, and Pradeep Khanna. "Wire arc additive manufacturing (WAAM): A new process to shape engineering materials." *Materials Today: Proceedings* 44 (2021): 118-128.
7. Chen, Xizhang, et al. "Cold metal transfer (CMT) based wire and arc additive manufacture (WAAM) system." *Journal of Surface Investigation: X-ray, Synchrotron and Neutron Techniques* 12 (2018): 1278-1284.
8. Jafari, Davoud, Tom HJ Vaneker, and Ian Gibson. "Wire and arc additive manufacturing: Opportunities and challenges to control the quality and accuracy of manufactured parts." *Materials & Design* 202 (2021): 109471.
9. Novelino, A. L. B., G. C. Carvalho, and M. Ziberov. "Influence of WAAM-CMT deposition parameters on wall geometry." *Advances in Industrial and Manufacturing Engineering* 5 (2022): 100105.
10. Singh, D. Dev, T. Mahender, and Avala Raji Reddy. "Powder bed fusion process: A brief review." *Materials Today: Proceedings* 46 (2021): 350-355.
11. Svetlizky, David, et al. "Directed energy deposition (DED) additive manufacturing: Physical characteristics, defects, challenges and applications." *Materials Today* 49 (2021): 271-295.
12. Derekar, K. S. "A review of wire arc additive manufacturing and advances in wire arc additive manufacturing of aluminium." *Materials science and technology* 34.8 (2018): 895-916.
13. Jafari, Davoud, Tom HJ Vaneker, and Ian Gibson. "Wire and arc additive manufacturing: Opportunities and challenges to control the quality and accuracy of manufactured parts." *Materials & Design* 202 (2021): 109471.
14. Vimal, K. E. K., M. Naveen Srinivas, and Sonu Rajak. "Wire arc additive manufacturing of aluminium alloys: a review." *Materials Today: Proceedings* 41 (2021): 1139-1145.
15. Qi, Zewu, et al. "Microstructure and mechanical properties of wire+ arc additively manufactured Al-Mg-Si aluminium alloy." *Materials Letters* 233 (2018): 348-350.
16. Gu, Jianglong, et al. "Wire+ arc additive manufacturing of aluminium." *2014 International Solid Freeform Fabrication Symposium*. University of Texas at Austin, 2014.
17. Ortega, Arturo Gomez, et al. "Characterisation of 4043 aluminium alloy deposits obtained by wire and arc additive manufacturing using a Cold Metal Transfer process." *Science and Technology of Welding and Joining* (2019).
18. Fang, Xuewei, et al. "Microstructure evolution of wire-arc additively manufactured 2319 aluminium alloy with interlayer hammering." *Materials Science and Engineering: A* 800 (2021): 140168.
19. Colegrove, Paul A., et al. "Microstructure and residual stress improvement in wire and arc additively manufactured parts through high-pressure rolling." *Journal of Materials Processing Technology* 213.10 (2013): 1782-1791.
20. Zhang, C., et al. "Strength improving mechanism of laser arc hybrid welding of wrought AA 2219 aluminium alloy using AlMg5 wire." *Science and Technology of Welding and Joining* 18.8 (2013): 703-710.